

## Optimization of the Isolation of Extracellular Vesicles via Dielectrophoresis: A preliminary Analysis

Nur Mas Ayu Jamaludin<sup>1</sup>, Muhammad Khairulanwar Abdul Rahim<sup>1</sup>, Azrul Azlan Hamzah<sup>1</sup>, Nadiah Abu<sup>2</sup>, and Muhamad Ramdzan Buyong<sup>1\*</sup>

<sup>1</sup>Institute of Microengineering and Nanotechnology, Universiti Kebangsaan Malaysia (UKM), 43600 Bangi, Malaysia.

<sup>2</sup> UKM Medical Molecular Biology Institute (UMBI), UKM Medical Centre, 56000 Cheras, Kuala Lumpur, Malaysia.

### ABSTRACT

*Extracellular vesicles (EVs); 30 nm to 1 micrometer in size; has gained its attention as their role as biomarkers and communicator from one cell to another. The importance of early detection for diseases is highly integral and key to patient's probability of survival. The drawback of many existing methods is that it can be time consuming and prone to false-negative results due to limitation of the circumstances. This research is aiming to address the disease detection technology limitation by using dielectrophoresis microelectrode principle to manipulate the properties of EVs. The important feature of dielectrophoresis is that this can be used as means to manipulate, transport and separate different types of particles, which one of them is EVs. Transmission Electron Microscopy (TEM) and Dynamic Light Scattering (DLS) has been used in this work to characterize the EVs. MATLAB provides the dielectrophoresis technique characterization for manipulation and separation of EVs from their medium. The EVs on the microelectrode has been supplied with 20 V peak-to-peak ( $V_{pp}$ ) for frequency in the range of 100 kHz to 10 Mhz to observe the DEP response. Figure 6 shows the movement of EVs at 100 kHz from the region of interest (ROI) to on top of the microelectrode which represents positive dielectrophoresis,  $P_{DEP}$ . The experimental testing shows its ability for this method to manipulate the EVs based on their physical characteristics and dielectric properties. Hence, the development of EVs manipulation using dielectrophoresis microelectrode technique offers a faster detection or diagnosis in the medical science field.*

**Keywords:** Biomarkers, Dielectrophoresis, Exosomes, Extracellular Vesicles.

### 1. INTRODUCTION

Extracellular vesicles or EVs are vesicle cells which are small in size that exists in the cellular systems in the form of multiple cell types. Due to their special attribute to serve as a 'carrier' that can move and exchange molecules, EVs have been studied extensively for the purpose of cell to cell communications. There are two categories of EVs. They are exosomes and microvesicles which are distinguished by their size and biogenesis mechanisms as shown in figure 1 [1], [2]. The most studied EVs is the exosomes which consists of a homogeneous cell of spherical vesicles which sized from 30 to 100 nm in diameter. The necessity for faster detection of diseases has increasingly become more important in the medical field to prevent casualties. The key to patients' probability of survival lies in the diagnosis being performed as early as possible [3]. The setback of finding the pathogen for these diseases is that they can be very time consuming. Furthermore, the nature of these tests is very expensive and difficult to run in small laboratory setup.

---

\*Corresponding Author: [muhdramdzan@ukm.edu.my](mailto:muhdramdzan@ukm.edu.my)

Early detection and technology for detecting diseases is highly important for patient's survival. There has been increasing interest of research about extracellular vesicles due to their potential; they have the properties for cell to cell communication and transmission of macromolecules [4]. Whilst the methods introduced such as electron microscopy is useful to characterize the EVs for the purpose of diagnosing or disease detection, these methods have limitations where it can be very time consuming and morphology needs to be modified for the preparation of the sample [5]. The dielectrophoresis microelectrode technique offers contactless method with no modification in the sample needed, and most importantly offers rapid and accurate real time detection [6].

Because of this, it is crucial to develop a diagnosis which are more accurate and quicker. The main interest of researchers in recent times has been in the field of distinguishing the properties between a healthy an unhealthy cell. A technique for this reason is utilized, called the dielectrophoresis (DEP) [7]. DEP is the phenomenon of generating neutral particle motion through the action of a non-uniform electrical field [8]–[13]. It describes in particular the motional behaviour of neutral matter as a result of exposure to a non-uniform electrical field in a given environment which induces particle repositioning to a new position. DEP has been widely used for the determination of cell, bacteria, virus, and protein based on the sample dielectric properties characteristics[14]–[17]. Dielectrophoresis capability in generated DEP forces, able to do the detection, manipulation, separation, and isolation of target cell from mixtures of different cells in aqueous suspension medium [18]–[20]. Therefore, we propose the DEP technique in manipulation and separation of EVs.

## 2. DIELECTROPHORESIS IN THEORY

Nonuniform electrical field subject to time-stationary (DC) or time-varying (AC) electrical field produced a net force intervening in the direction of locations relevant to the matter's polarization properties. Dielectrophoresis is the motion or particles and cells in a non-uniform electrical field, which was first observed by Pohl and most recently by R. Pethig. In an electric field,  $E$ , a dielectric particle functions as an effective dipole moment,  $p$ , in relation to the electric fields, which can be expressed as,

$$p \propto E \quad (1)$$

The proportional constant relies, in general, on the dielectric particle geometry. The force on a dipole is imposed in the presence of an electric field gradient, that is,

$$F = (p \cdot \nabla) E \quad (2)$$

where  $p$  is the vector of the constant dipole moment,  $\nabla$  is the vector of del and the external electrical field is  $E$ . The combination of the two equations is given by the ( $F_{DEP}$ ) for homogeneous particles suspended in electric field gradient;

$$F_{DEP} = 2 \pi \varepsilon_{medium} R^3 CMF (\nabla E^2) \quad (3)$$

where  $r$  is the radius of particle,  $\varepsilon_{medium}$  is the permittivity of the suspending medium and  $\nabla E$  is the gradient of the rms electric field. Thus, the real part of the Clausius-Mossotti factor is given by,

$$CMF = \frac{(\varepsilon_{particle} - \varepsilon_{medium})}{(\varepsilon_{particle} + 2\varepsilon_{medium})} \quad (4)$$

where  $\epsilon_{particle}$  and  $\epsilon_{medium}$  are the complex permittivities of the particles or cells and medium.

For implementations of DEP for detection of EVs, we need to characterize the dielectric properties for phenotype and physiological state of EVs and surrounding medium. The dielectric property of EVs is defined as physical structure (referred to exterior) and chemical composition (referred to interior). Based on unique EVs identifications, external morphologies of the physical structure are later converted into dielectric properties. The dynamic dielectric properties consisting of resistance and conductance that is the permittivity and conductivity value of EVs will fluctuate based on the frequency of inputs. The fluctuation of dielectric properties causes DEP force to be produced, either attraction or repulsion forming a high intensity of the electric field. The novelty of this microelectrode platform at the bottom edge and top edge of the sidewall taper electrode generated two spot intensity electric field. The benefits, due to lateral force attraction and/or vertical force repulsion for targeted particle, we are able to do manipulation and separation at two different locations.

The co-relation of the permittivity and conductivity value of EVs, which provides an understanding of the electrical properties dependent on frequency. With increasing frequency, the observed increase in the effective conductivity. The huge relative permittivity values are shown at the lower frequencies reflect the multitude of polarization between the interfaces. Polarization charges can only accumulate on an EVs' surface, as long as it acts as an electrical insulator. This is possible at low frequencies because the surface capacitance reaction is too high to provide the accumulated ions with a path of leakage. The effective impedance to charge leakage presented by the parallel combination of surface resistance and capacitance is reduced with increasing frequency, and with this, the interfacial polarization and effective permittivity are also reduced.

In DEP-based manipulations, the detection response of EVs is primarily defined by their exterior morphological characteristics. As a result, DEP can discriminate between EVs of similar size having different morphological origins, offering only a substantial advantage over size.

### **3. MATERIAL AND METHODS**

#### **3.1 Sample Preparation and Characterization**

In this work, EVs recovered from colorectal cancer, SW480; used as the targeted EVs. This sample was obtained from one of the authors. These unique attributes are important to characterize this uniqueness to their own dielectric properties. Characterization of physical properties of EVs are very crucial for the modelling of dielectric dynamic of dielectrophoresis technique using MATLAB analytical software for manipulation and separation of EVs from their medium.

Transmission Electron Microscopy (TEM) took place for the EVs to observe the size of EVs. The EVs undergo staining and dilution with 1:1 ratio; the ratio of EVs to the deionized (DI) water. The staining method starts with a droplet of EVs on formvar grid and stained with 3% uranyl acetate for 5 minutes. It was then washed three times with distilled water. The EVs was left to dry on the formvar grid overnight and was viewed with TEM.

DLS has recently been exploited to characterize the distribution of the size of the EVs [21], [22]. In DLS, fluctuations of the scattered light intensity are correlated to obtain information about particle size due to the Brownian motion of the particles. As DLS is non-invasive, extremely reactive, and needs relatively low quantities of tests, it is commonly used in many research fields.

Indeed, DLS's simplicity and ease of use made it the gold standard for determining the size distribution of suspensions quickly and accurately [23]–[25]. The EVs sample was diluted with a ratio of 1:300, which reflects the sample-to-medium ratio of deionized water (DI water) used in this research. The data was obtained using a dip cell cuvette and submerged in a 1500  $\mu\text{l}$  water to be used with Zetasizer Nano ZS (Malvern Devices, Malvern, UK) fitted with 633 nm He-Ne laser and 173° operating angle.

### 3.2 EVs Numerical Analysis

Next, this work is going to report on characterization of dielectrophoresis technique using MATLAB analytical for manipulation and separation of EVs from their medium. Evaluation of polarization factor and dielectric dynamic properties between EVs and medium are related to the value of permittivity ( $\epsilon$ ) and conductivity ( $\sigma$ ) by using MATLAB analytics software. Change of polarization and change of dynamics dielectric factor for EVs are response due to input frequencies by alternating current source to dielectrophoresis electrode. Based on the polarization factor, the new average value of the optimal crossover frequencies is obtained. It aims to produce optimum  $F_{\text{DEP}}$  which is the optimum  $P_{\text{DEP}}$  force and optimum  $N_{\text{DEP}}$  force against targeted particles and vice versa.

Then, the CMF factor of EVs obtained from MATLAB simulation was validated using existing dielectrophoresis electrode. This experimental are consists of qualitative (visualize via microscopy) and quantitative (response of input frequencies to EVs CMF factor). This visualize technique most important for observe which region the EVs movement on DEP electrode either  $P_{\text{DEP}}$  or  $N_{\text{DEP}}$  response.

### 3.3 Experimental Setup

Moving forward, the experimental testing setup as shown in figure 2 with dielectrophoresis microelectrode with tapered profile of 70° has been built to perform the electric field manipulation on the EVs on the region of interest [26]. The EVs has been stained using PKH26 (MINI26–1KT), a red membrane dye (Sigma-Aldrich, St. Louis, MO, USA) since the experimental setup is conducted under fluorescent microscope as the solution for nano size particles used in this study. Fluorescent microscope (BA400; Motic, Wetzlar, Germany) with 40x magnification and was equipped with Dinoeye Eyepiece microscope camera (Dino-lite, Torrance, CA). The microscope needs to be set to the correct wavelength according to the dye specifications. 1  $\mu\text{L}$  of EVs was dropped on the microelectrode and covered by a 1 mm glass slide. The microscope needs to be adjusted according to the ROI. A sinusoidal alternating current (AC) with 20 V peak-to-peak ( $V_{\text{pp}}$ ) was supplied by function generator using prober onto the pad. Input frequency ranging from 100 kHz to 10 MHz were used to see both  $P_{\text{DEP}}$  and  $N_{\text{DEP}}$ .

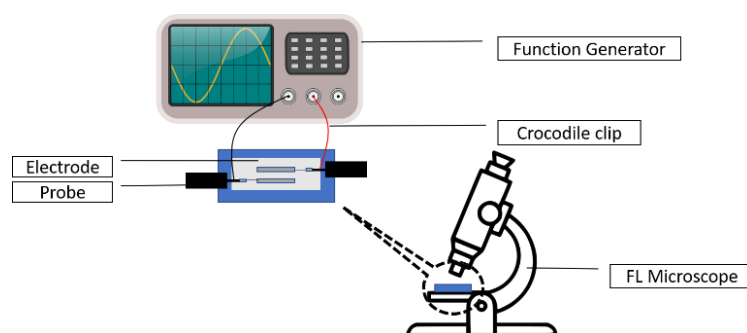


**Figure 1.** The dielectrophoresis experimental setup.

### 3.3 Movement of EVs

Figure 2 shows the EVs behaviour towards  $F_{DEP}$  manipulation. Exosomes (30-100 nm) and microvesicles (100-1000 nm) which both present in EVs, can be manipulated using the concept of  $P_{DEP}$  and  $N_{DEP}$ . Figure 2 (a) shows the region of interest (ROI) where the electric field exist when different potential is given towards the microelectrode [27]. In Figure 2 (b), the EVs will be manipulated and then separated according to the input frequency supplied as illustrated in the figure. Finally, both exosomes and microvesicles were separated, exosomes were in  $P_{DEP}$  region and microvesicles were in  $N_{DEP}$  region as shown in Figure 2 (c).

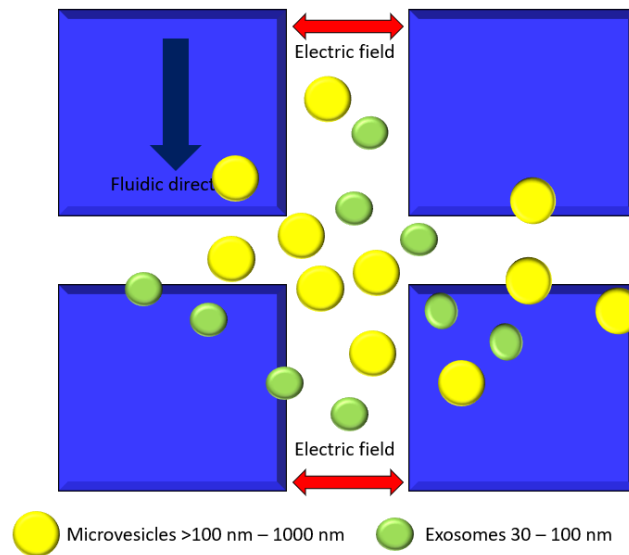


**Figure 2 (a).** The mechanism of  $F_{DEP}$  manipulation towards EVs consists of exosomes and MVs are scattered on the microelectrode.

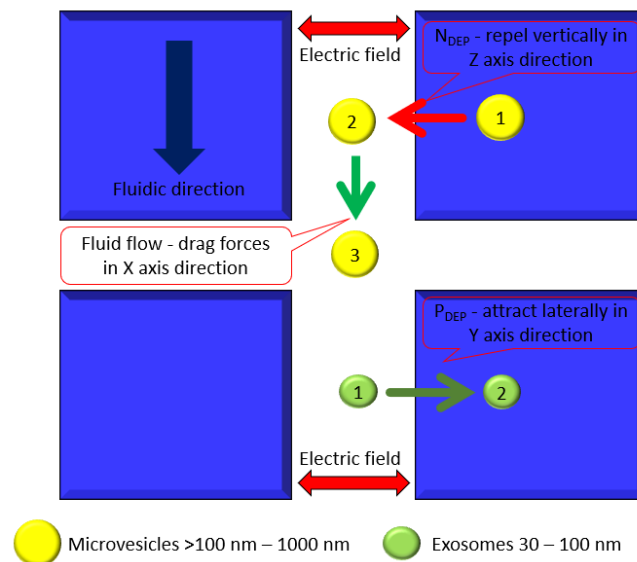


**Figure 2 (b).** Repel and attract movement due to electric field produced by voltage supplied.

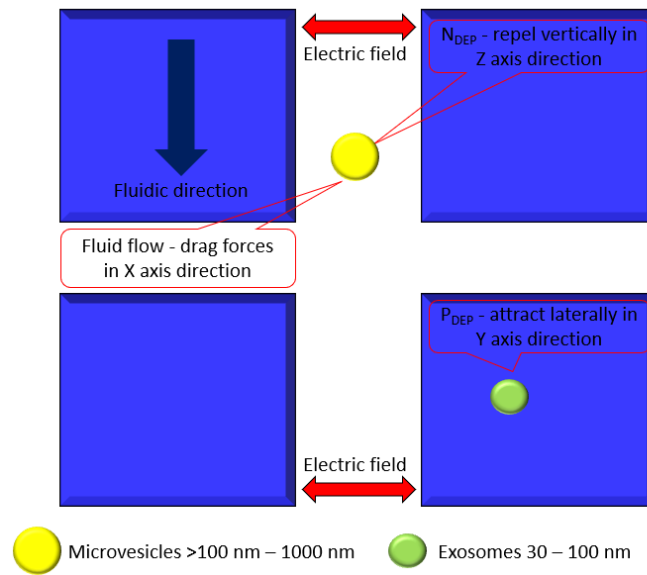


**Figure 2 (c).** Positions of EVs after electric field applied.

## 4. RESULTS AND DISCUSSION

### 4.1 Transmission Electron Microscopy (TEM)

Figure 3 shows the size of a single exosomes; which confirmed by the size range; obtained from TEM characterization with the average size of 42 nm in diameter. From this TEM result, it shows that the EVs are in spherical shape with membrane. From the TEM results, it shows that two populations are present in the EVs sample used in this work. Thus, it proves the heterogeneity of EVs as per mentioned before.

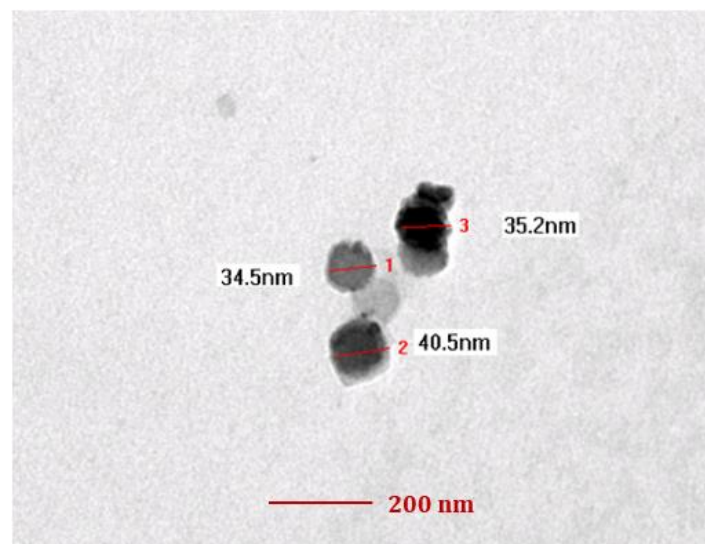


**Figure 3 (a).** Images of EVs from transmission electron microscopy (TEM) of exosomes population.

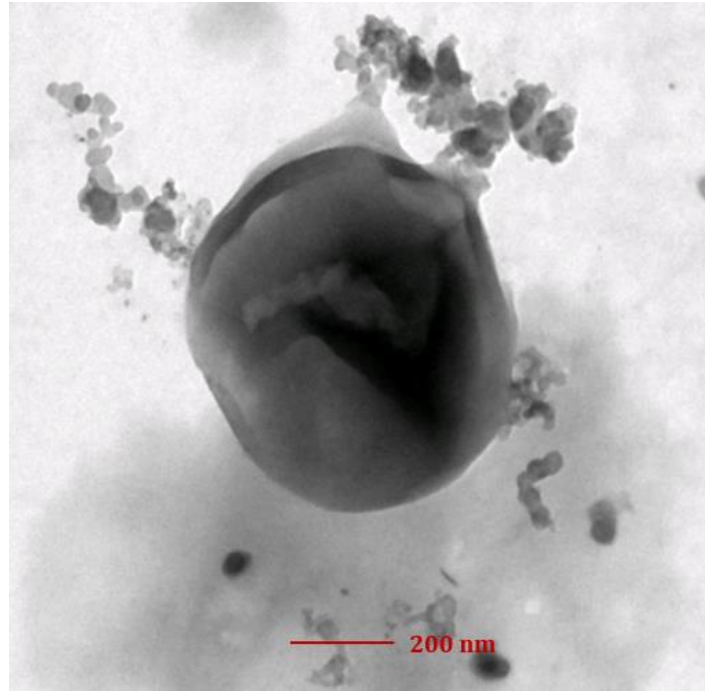


**Figure 3 (b).** Images of EVs from transmission electron microscopy (TEM) of microvesicles population.

#### 4.2 Dynamic Light Scattering (DLS)

The EVs then undergo the characterization by using Dynamic Light Scattering (DLS) method. The graph was produced after the sample was tested using the Zetasizer Nano ZS (Malvern Devices, Malvern, UK). The software provided by the Malvern Instruments Ltd. was able to plot the graph of the two populations in EVs as shown in figure 4 below. The population of microvesicles are higher than the population of exosomes. The peak value of MVs is at 241 nm in diameter while the peak value of exosomes is at 44 nm in diameter.

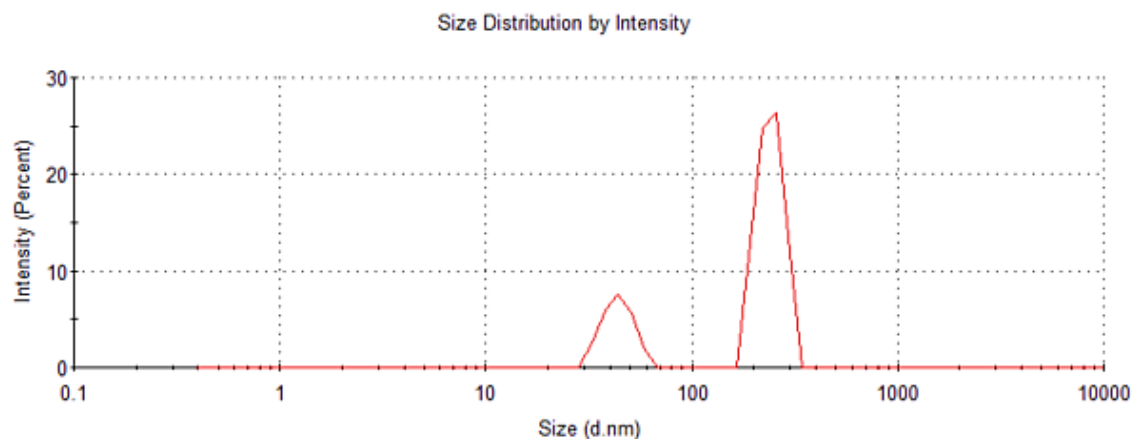


**Figure 4.** Result obtained from Zetasizer on size distribution of EVs by intensity in percent.

#### 4.3 Clausius-Mossotti Factor (CMF) of EVs

Next, in this analytical characterization as shown in figure 5, biological cell which is EVs with its medium; phosphate-buffered saline (PBS) was used. The conductivity and the permittivity of PBS which are  $\sigma = 1.4 \text{ S m}^{-1}$  and  $\epsilon = 80$ .

Figure 5 (a) explains the attraction force of  $P_{DEP}$  to repulsion force of  $N_{DEP}$ . This is explained by the low input frequency values before the crossover frequency value of exosomes is exposed to the  $P_{DEP}$  attractive forces. After the crossover frequency values, exosomes on high input frequency value is exposed to  $N_{DEP}$  repulsive forces. The midpoint of transaction forces between  $P_{DEP}$  to  $N_{DEP}$  is  $F_{DEP} = 0$ .  $F_{DEP}$  is zero because the  $P_{DEP}$  attractive forces to  $N_{DEP}$  repulsive forces are equal.

Figure 5 (b) and figure 5 (c) shows the conductivity and permittivity response of exosomes and PBS in response to the input frequency values which both results are combined in figure 5 (d). The comparison of both results that explains the change in permittivity value between exosomes and PBS with the increase of frequency input value. The permittivity value of exosomes and PBS intersection point are at the crossover frequency point. This means that the exosomes permittivity value and PBS is the same at that point. This explains the main factor of the change in permittivity value and media as reaction to the increase in frequency input value.

Next, it also explains the conductivity value between exosomes and PBS with the increase of frequency input value. The combination between these two changes with the input frequency values. Intersection point of the conductivity between exosomes and PBS are at the crossover frequency point. This shows the conductivity values of exosomes and PBS are same in response to the increasing of input frequency values.

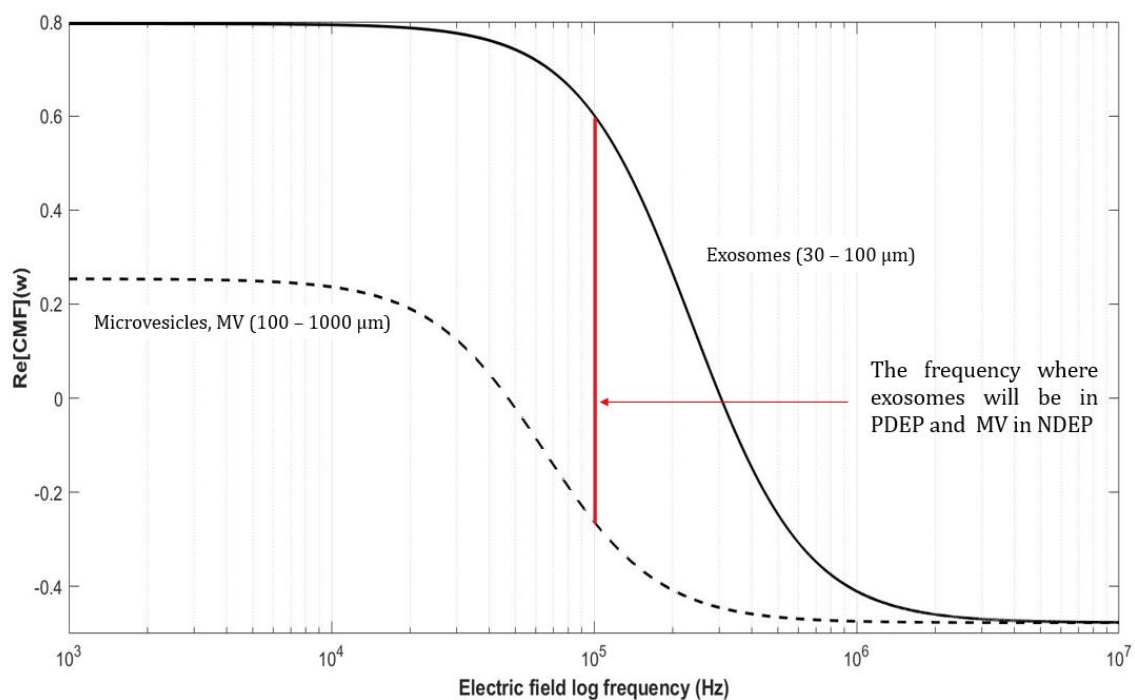


**Figure 5 (a).** The graph of attraction force of  $P_{DEP}$  to repulsion force of  $N_{DEP}$ . The graph represents two population of EVs.



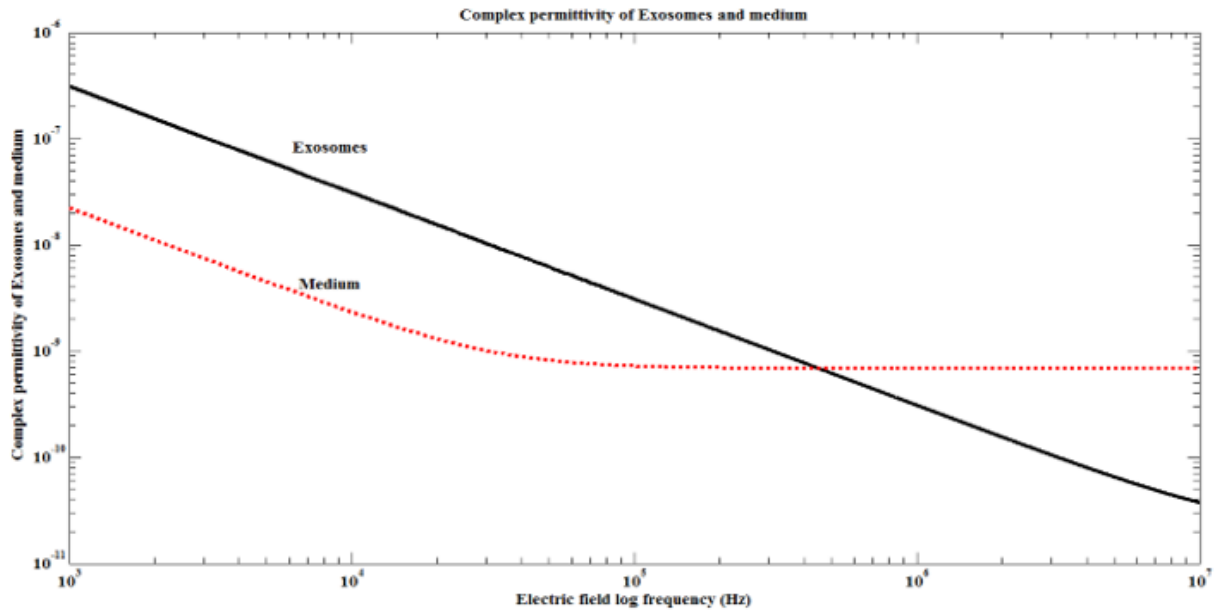


Figure 5 (b). The graph of complex permittivity of exosomes and medium.

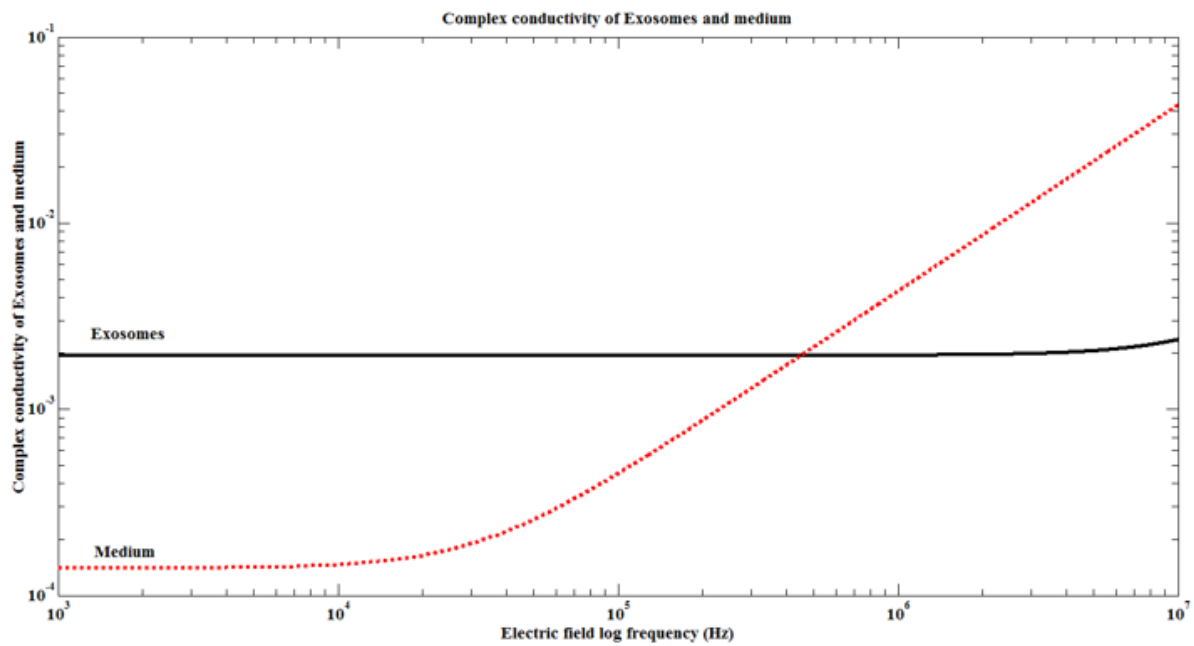


Figure 5 (c). The graph of complex conductivity of exosomes and medium.

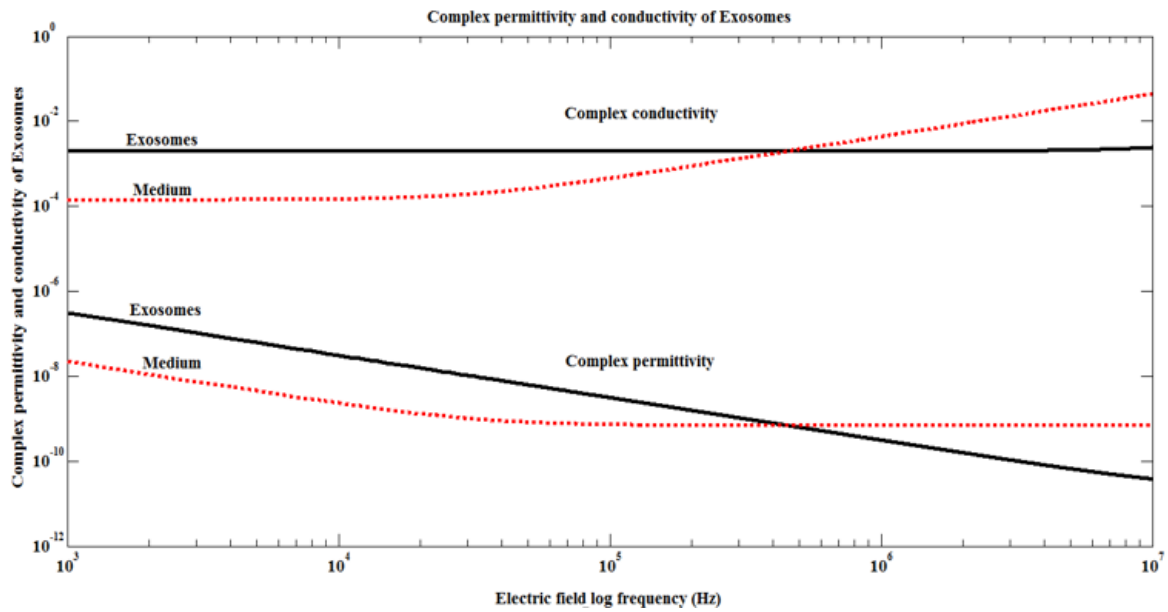


Figure 5 (d). The graph of complex permittivity and conductivity of exosomes.

#### 4.4 Experimental Result

From the previous analytical modelling results, the EVs was then undergoing the experimental testing to test the effect of input frequency and voltage towards the dielectrophoretic manipulation. In figure 6, the image of EVs after applying 100 kHz at 20 V peak-to-peak ( $V_{pp}$ ). Initially, all EVs are scattered across the ROI. After the selected frequency has been applied, the EVs are attracted from the ROI to the top surface of microelectrode as shown from the figures below. It can be said that the EVs was attracted onto the electrode which conclude it as positive dielectrophoresis,  $P_{DEP}$  which are the lateral attraction of the EVs. This explains the graph obtained in figure 5 on how low input frequency will give the results of  $P_{DEP}$ .

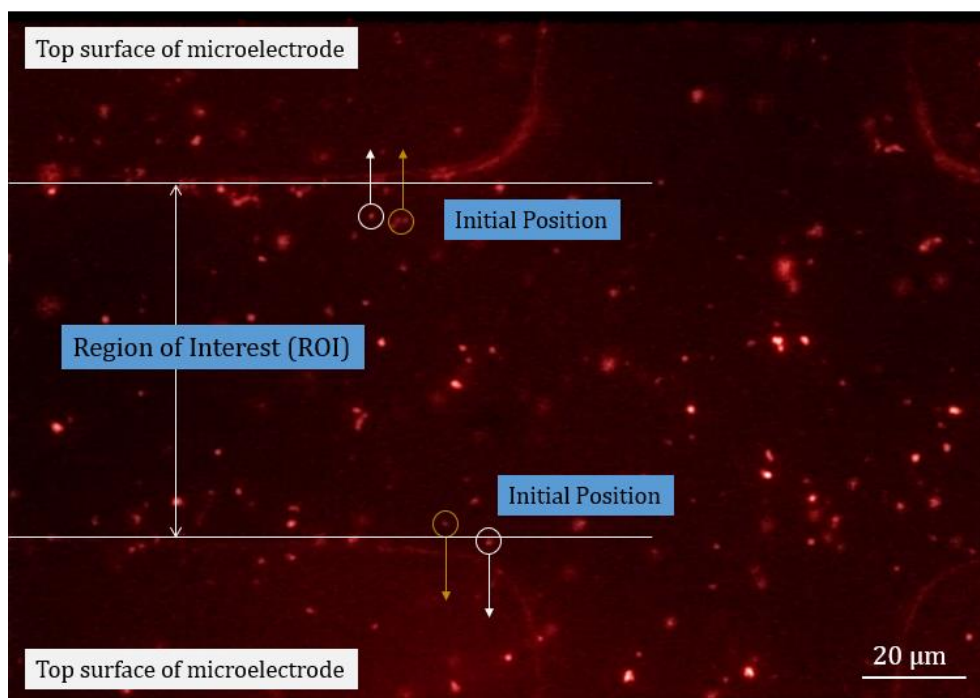
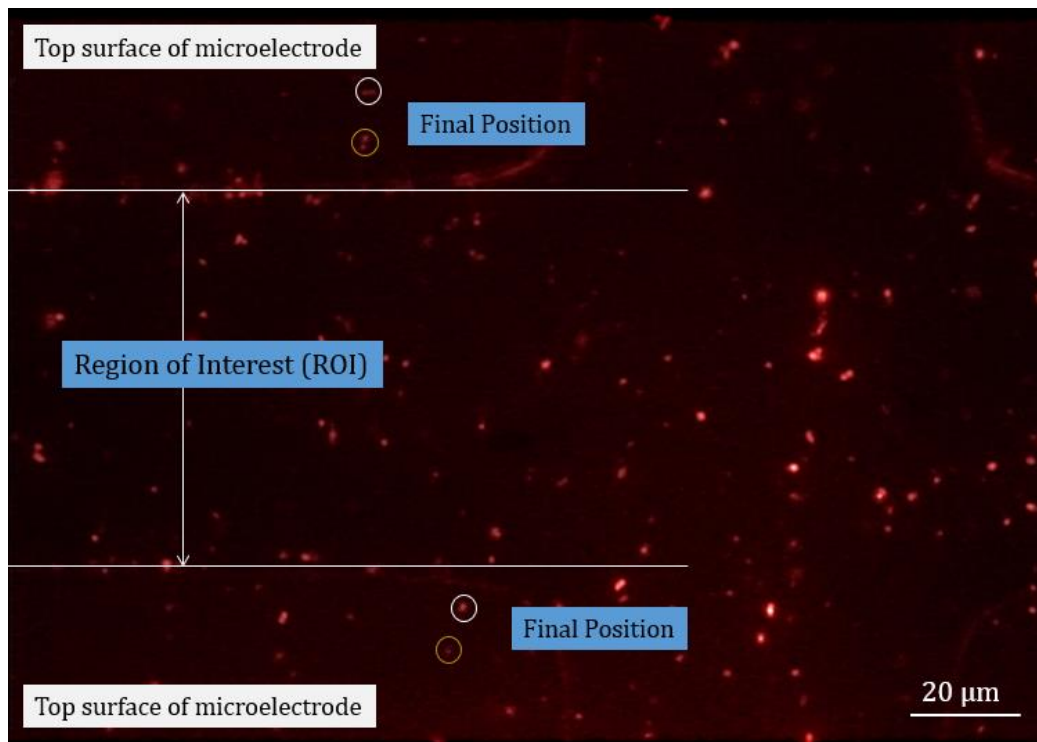


Figure 6 (a). The initial position of targeted EVs on the ROI.



**Figure 6 (b).** The final position of targeted EVs after 10 second applying 100 kHz at 20  $V_{pp}$ .

## 5. CONCLUSION

In conclusion, EVs have undergone sample preparation and characterization to see the populations of the EVs used in this work. The numerical analysis was crucial to understanding the co-relation of the permittivity and conductivity value of EVs, which provides an understanding of the electrical properties dependent on frequency. The experimental setup was set to perform the DEP technique towards the EVs. The results of TEM and DLS proves the heterogeneity of EVs; exosomes and MVs were present. Next, the CMF factor shows the ability of this technique to be used in the manipulation and separation of EVs. At 100 kHz of input frequency with 20 Vpp, the EVs experiencing lateral attraction where the movement of EVs from the ROI to the top surface of the microelectrode. Hence, this proves the theory of the CMF factor;  $P_{dep}$  was present at the stated input frequency. The potential was addressed clearly, which provides promising for the in-situ monitoring of EVs by using the DEP technique.

## ACKNOWLEDGEMENTS

The author would like to acknowledge with gratitude the sponsor of Dana Cabaran Perdana (DCP-2017-003/3) funded by Universiti Kebangsaan Malaysia (UKM) as a Research University and AKU254: HICOE (FASA2) for Artificial Kidney grant funded by the Ministry of Higher Education (MOHE) Malaysia. The author would also like to thank Mrs. Suhada Binti Mansor (Jabatan Patologi) and Mr. Mohd Harisfazal Bin Mohamed Basri (Jabatan Perkhidmatan Makmal Diagnostik) from Pusat Perubatan Universiti Kebangsaan Malaysia (PPUKM) for their services.

## REFERENCES

- [1] M. C. Cufaro *et al.*, "Extracellular Vesicles and Their Potential Use in Monitoring Cancer Progression and Therapy : The Contribution of Proteomics," **2019** [2019].
- [2] W. Wang, J. Luo, & S. Wang, "Recent Progress in Isolation and Detection of Extracellular Vesicles for Cancer Diagnostics," **1800484** 1–27 (2018).
- [3] I. J. Jacobs & U. Menon, "Progress and Challenges in Screening for Early Detection of Ovarian Cancer \*," 355–366 [2004].
- [4] J. R. Edgar, "Q & A : What are exosomes , exactly ?," BMC Biol. 1–7 [2016].
- [5] B. A. Ashcroft, J. De Sonnevile, Y. Yuana, & S. Osanto, "Determination of the size distribution of blood microparticles directly in plasma using atomic force microscopy and microfluidics," 641–649 [2012].
- [6] P. R. C. Gascoyne & S. Shim, "Isolation of circulating tumor cells by dielectrophoresis," *Cancers (Basel)*. **6**, 1 [2014] 545–579.
- [7] N. A. Rahman, F. Ibrahim, & B. Yafouz, "Dielectrophoresis for Biomedical Sciences Applications : A Review," 1–27 [2017].
- [8] R. Pethig, "Dielectrophoresis: An assessment of its potential to aid the research and practice of drug discovery and delivery," *Adv. Drug Deliv. Rev.*, [2013].
- [9] D. Peyrade, "Moving pulsed dielectrophoresis Lab on a Chip," no. February 2013 (2014).
- [10] K. Khoshmanesh, S. Nahavandi, S. Baratchi, A. Mitchell, & K. Kalantar-zadeh, "Biosensors and Bioelectronics Dielectrophoretic platforms for bio-microfluidic systems," *Biosens. Bioelectron.* **26**, 5 (2011) 1800–1814.
- [11] R. Pethig, "Review Article — Dielectrophoresis : Status of the theory , technology , and applications," 1–35 [2010].
- [12] R. Pethig, A. Menachery, S. Pells, & P. De Sousa, "Dielectrophoresis : A Review of Applications for Stem Cell Research," **2010** (2010).
- [13] H. A. Pohl & K. Pollock, "Dielectrophoretic Force : A Comparison of Theory and Experiment," 133–134 [1979].
- [14] N. M. A. Jamaludin, M. R. Buyong, M. K. A. Rahim, A. A. Hamzah, B. Y. Mailis, & B. Bais, "Dielectrophoresis: Characterization of triple-negative breast cancer using clausius-mossotti factor," *IEEE Int. Conf. Semicond. Electron. Proceedings, ICSE 2018-Augus* (2018) 85–88.
- [15] M. K. A. Rahim, M. R. Buyong, N. M. A. Jamaludin, A. A. Hamzah, K. S. Siow, & B. Y. Majlis, "Characterization of permittivity and conductivity for ESKAPE pathogens detection," *IEEE Int. Conf. Semicond. Electron. Proceedings, ICSE 2018-Augus* (2018) 132–135.
- [16] F. W. Yunus, A. A. Hamzah, M. S. Norzin, M. R. Buyong, J. Yunas, & B. Y. Majlis, "Dielectrophoresis: Iron deficient anemic red blood cells for artificial kidney purposes," *IEEE Int. Conf. Semicond. Electron. Proceedings, ICSE 2018-Augus* (2018) 5–8.
- [17] M. I. Abd Samad, M. R. Buyong, S. S. Kim, & B. Yeop Majlis, "Dielectrophoresis velocities response on tapered electrode profile: simulation and experimental," *Microelectron. Int.* **36**, 2 (2019) 45–53.
- [18] K. F. Hoettges, Dielectrophoresis as a Cell Characterisation Tool **583** [2010].
- [19] N. Piacentini, G. Mernier, R. Tornay, P. Renaud, & P. Renaud, "Separation of platelets from other blood cells in continuous-flow by dielectrophoresis field-flow- fractionation," **034122**, 2011 (2014).
- [20] S. Shim *et al.*, "Dielectrophoresis has broad applicability to marker-free isolation of tumor cells from blood by microfluidic systems," **011808** (2013).
- [21] V. Filipe, A. Hawe, & W. Jiskoot, "Critical Evaluation of Nanoparticle Tracking Analysis (NTA) by NanoSight for the Measurement of Nanoparticles and Protein Aggregates," *Pharm. Res.* **27**, 5 (2010) 796–810.
- [22] A. S. Lawrie, A. Albanyan, R. A. Cardigan, I. J. MacKie, & P. Harrison, "Microparticle sizing by dynamic light scattering in fresh-frozen plasma," *Vox Sang.* **96**, 3 (2009) 206–212.

- [23] F. Andreasi Bassi, G. Arcovito, M. De Spirito, A. Mordente, & G. E. Martorana, "Self-similarity properties of alpha-crystallin supramolecular aggregates," *Biophys. J.* **69**, 6 (1995) 2720–2727.
- [24] T. Parasassi *et al.*, "Low density lipoprotein misfolding and amyloidogenesis," *FASEB J.* **22**, 7 (2008) 2350–2356.
- [25] G. Maulucci, M. De Spirito, G. Arcovito, F. Boffi, A. C. Castellano, & G. Briganti, "Particle Size Distribution in DMPC Vesicles Solutions Undergoing Different Sonication Times," *Biophys. J.* **88**, 5 (2005) 3545–3550.
- [26] M. R. Buyong, F. Larki, M. S. Faiz, A. A. Hamzah, J. Yunas, & B. Y. Majlis, "A Tapered Aluminium Microelectrode Array for Improvement of Dielectrophoresis-Based Particle Manipulation," (2015) 10973–10990.
- [27] M. R. Buyong, F. Larki, Y. Takamura, & B. Y. Majlis, "Tapered microelectrode array system for dielectrophoretically filtration: fabrication, characterization, and simulation study," **16** (2017) 44501–44508.

